PHASE COHERENCE IN CLASSICAL AND QUANTUM SUPERCONDUCTING ARRAYS

Beom Jun Kim
Department of Theoretical Physics, Umeå University, 901 87 Umeå, Sweden

Gun Sang Jeon
Center for Strongly Correlated Materials Research, Seoul National University, Seoul, 151-747, Korea

M. Y. Choi
Department of Physics, Seoul National University, Seoul 151-747, Korea

1 INTRODUCTION

Quantum mechanics, which is quite successful in describing the physics in the microscopic scale such as electrons in an atom, tells us that particles interfere with each other due to their inherent wave nature. However, such phenomena are rarely observed in a macroscopic system, which has made the basic concepts of the quantum theory difficult to accept. As we understand, the main reason is that a macroscopic system is inevitably coupled to the environment composed of many microscopic degrees of freedom. It is generally believed that this coupling to the environment introduces dissipation effects and makes the macroscopic system lose its quantum coherence; this is the orthodox answer to the question why we do not see the Schrödinger cat in everyday life. Such a macroscopic system, where quantum coherence is absent, is well described by classical statistical mechanics, and many interesting physical properties including critical phenomena may be studied with thermal fluctuations solely (but not quantum fluctuations) taken into consideration. On the other hand, in some systems like superconductors, dissipation is sufficiently weak and quantum effects can be observed. Also at very low temperatures, a small system can maintain quantum coherence since the coherence length becomes longer than the system size. Such mesoscopic systems are in-between the microscopic and

the macroscopic systems and thus useful to understand quantum and statistical physics in different scales. In addition, they are becoming more and more important in the practical sense because recent development of the nano-technology makes it possible to fabricate mesoscopic devices, where consideration of quantum effects is crucial [1].

In this article, we study the two-dimensional (2D) superconducting arrays, composed of many periodically arranged superconducting grains each of which is coupled to other neighboring grains by the Josephson effect [for the superconducting-insulating-superconducting (S-I-S) type junction] or the proximity effect [for the superconducting-normal-superconducting (S-N-S) junction] [2]. These effects make it possible that the superconducting grains behave in a cooperative manner to establish phase coherence across the entire system and to display many interesting collective phenomena. For example, at sufficiently low temperatures, the 2D Josephson junction array (JJA) becomes superconducting as a whole, although each superconducting grain is separated by the normal (or insulating) material. They are also very important from the experimental point of view since theoretical predictions and experimental observations can be compared with each other in a controllable way.

In addition to the coupling energy, there exists the charging energy, associated with the capacitance of the superconducting grains. When the size of each superconducting grain is not too small, however, the capacitance is rather large and makes the charging energy, inversely proportional to the capacitance, negligibly small. In this case, although the superconductivity itself is a quantum mechanical phenomenon, the cooperative phenomena in superconducting arrays are governed by thermal fluctuations and thus described by classical statistical mechanics. For those "classical arrays", where charging energy can be neglected, many interesting equilibrium and dynamic properties have been intensively studied. In particular external magnetic fields introduce *frustration* to the system, bringing about rich physics: Concerning equilibrium transitions, the celebrated Berezinskii-Kosterlitz-Thouless (BKT) transition [3] has been observed and investigated in detail, the Ising-type transition has also been suggested, and there have been predictions of a reentrant transition as well as a glass transition. Dynamic transport properties such as the current-voltage characteristics, dynamic resistances, voltage and flux noise spectra, giant Shapiro steps, and the stochastic resonance have been proposed and investigated widely in a number of studies. It is also of interest that within the mean-field approximation the superconducting arrays under external magnetic fields can be mapped onto the tight-binding electron systems. This suggests that the superconducting array can be used to study interesting phenomena which have counterparts in electron systems.

In recent years, thanks to the state-of-the-art microfabrication technique, it becomes possible to fabricate a superconducting array, where the size of the grain is so small that the charging energy may not be neglected any more, in comparison with the Josephson coupling energy. Similarly to the Coulomb blockade effects during single electron tunneling in electron systems, which reflects discreteness of the elementary electron charge, the superconducting arrays with non-negligible charging energy can display the Coulomb blockade effects of the Cooper pairs. In these

"quantum arrays", the number of Cooper pairs on each grain may be regarded as the quantum mechanical variable conjugate to the phase of the superconducting condensate. Thus the effects of quantum fluctuations become important and the classical description is not valid any more [4]. Furthermore, the gauge charge induced from the gate voltage introduces another kind of frustration in addition to the frustration due to the external magnetic field, which is present in the classical arrays as well. Accordingly, such quantum arrays exhibit transitions from the superconducting phase to the normal or the insulating phase, together with rich behavior, arising from the interplay of thermal and quantum fluctuations. Superconducting arrays in the quantum regime can also be mapped onto other interesting quantum systems such as the charge-density wave system, the Bose-Hubbard model, and the quantum spin model in appropriate limits. Particularly, in two dimensions, through the use of the dual transformation, one can describe the system in terms of the vortex degrees of freedom instead of Cooper pair charges. The physical properties of the arrays can then be understood by the statics and dynamics of the vortices.

It is well known that quantum coherence in electron systems produces a variety of interesting quantum phenomena. The counterparts in the superconducting arrays can be observed, manifesting quantum coherence in the array systems. Among those suggested and/or experimentally observed are persistent currents, localization effects, Bloch oscillations, inverse Shapiro steps, the quantum Hall effect, and quantum chaos. In addition, one can also study a number of interesting phenomena such as the persistent voltage, the Aharonov-Casher effect, macroscopic quantum phenomena in the presence of dissipation, Bose-Einstein condensation, and quantum phase transitions.

This article is organized in the following way: In Sec. 2 we review the physical properties of classical superconducting arrays, with emphasis on the phase transitions and various dynamical behaviors. Section 3 is devoted to the discussion of the quantum effects in the superconducting array. Finally, Sec. 4 presents a brief conclusion.

2 CLASSICAL ARRAYS

When the size of the superconducting grains constituting the superconducting array is not larger than the Ginzburg-Landau (GL) coherence length, the superconducting order parameter Ψ may be considered to be uniform inside each grain. In this case, the GL free energy functional, which reads [5]

$$F = \int d\mathbf{r} \left[a|\Psi(\mathbf{r})|^2 + \frac{b}{2}|\Psi(\mathbf{r})|^4 + c|\nabla\Psi(\mathbf{r})|^2 \right] \tag{1}$$

for a bulk superconductor in continuum, can be cast into the discretized form

$$F = \sum_i \left[a|\Psi_i|^2 + \frac{b}{2}|\Psi_i|^4 \right] + 2c \sum_{\langle i,j \rangle} |\Psi_i - \Psi_j|^2, \tag{2}$$

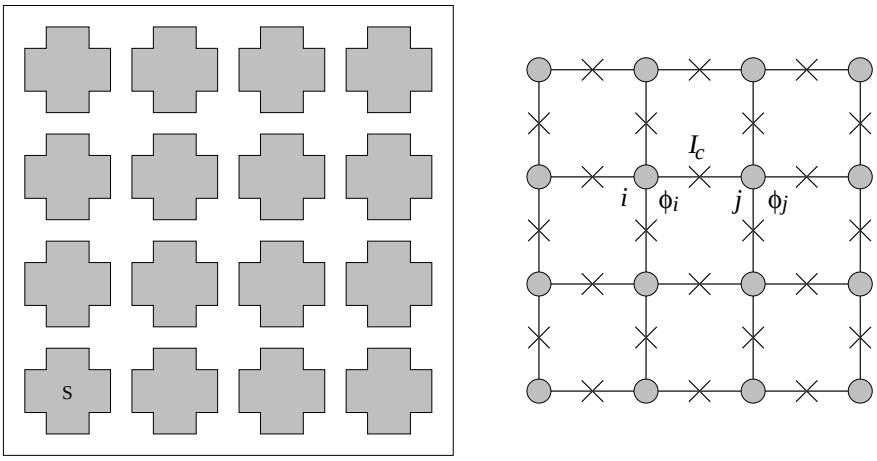

Figure 1: A schematic diagram of the two-dimensional square superconducting array or the Josephson-junction array. Superconducting grains (marked with "S") are placed on the substrate which is either a normal metal or an insulator. When the separation between neighboring grains is small enough, each grain is coupled to neighboring ones by the Josephson coupling. The figure in the right-hand side represents the corresponding model system, where the amplitude fluctuations of the complex order parameter are neglected and thus the grain at site i is described solely by the phase variable ϕ_i. The cross symbols between grains denote the Josephson coupling with the critical current I_c.

where $\Psi_i \equiv |\Psi_i|e^{i\phi_i}$ is the complex superconducting order parameter at the ith grain and the last term is the discretized expression of the gradient energy with the sum over nearest neighboring pairs (without double counting). The parameters b and c are positive, whereas a depends upon the temperature T, satisfying $a > 0$ for $T > T_0$, $a < 0$ for $T < T_0$, and $a = 0$ at the Bardeen-Cooper-Schrieffer (BCS) transition temperature T_0 [5]. The system described by the above GL free energy functional undergoes two distinct phase transitions. The first one at higher temperature T_0 is related with the appearance of the nonzero amplitude of the order parameter: For $T > T_0$ F has a minimum when $|\Psi_i| = 0$, while $|\Psi_i| = \sqrt{-a/b} \neq 0$ gives the minimum of F for $T < T_0$, implying that below the BCS transition temperature each grain of the array becomes superconducting. However, phases of the superconducting order parameters are still uncorrelated across the system. Accordingly, the whole system is not superconducting yet and remains normal until the other transition temperature $T_c(< T_0)$ is reached from above.

Below the lower transition temperature T_c, the system acquires global phase coherence and finally behaves as a superconductor. In general, T_c is well separated from T_0 and the perturbative approach indicates that amplitude fluctuations are irrelevant in the renormalization group sense, not changing the qualitative behavior of the system near T_c. In this respect, one can assume that $|\Psi_i|$ is constant and neglect the first two terms in Eq. (2), to obtain the effective Hamiltonian in the

same form as the classical XY model:

$$H = -E_J \sum_{\langle i,j \rangle} \cos(\phi_i - \phi_j), \tag{3}$$

where ϕ_i is the phase of the complex order parameter at site i and $E_J \equiv 2c|\Psi|^2$ [see Eq. (2)]. The above Hamiltonian can also be derived from the Josephson relations applied to the JJA, and one can relate the Josephson coupling strength E_J to the critical current I_c of the individual junction, i.e., $E_J = (\hbar/2e)I_c$. (See Fig. 1 for the schematic diagram of a JJA).

In three dimensions the system described by the Hamiltonian in Eq. (3) acquires, via a usual continuous phase transition, phase coherence or off-diagonal long-range order at low temperatures [6]; this is appropriate for describing the superfluid transition in the bulk liquid Helium [7]. In two dimensions, on the other hand, according to the Mermin-Wagner theorem [8], continuous symmetry such as the $U(1)$ symmetry in this case cannot be broken in the system with short-range interactions. However, it has been shown later [3] that in spite of the absence of true long-range order, the correlation function, defined to be $\Gamma(r) \equiv \langle e^{i(\phi_i - \phi_j)} \rangle$ with the ensemble average $\langle \cdots \rangle$ and the separation r between the sites i and j, changes its behavior qualitatively as T is lowered: Whereas at $T > T_c$, $\Gamma(r)$ decays exponentially, it displays algebraic decay at $T < T_c$. Such algebraic decay is extremely slower than the exponential one and has no finite characteristic length scale, and the system is considered to have quasi-long-range order.

The continuum version of Eq. (3) reduces to the Hamiltonian for the Gaussian model, taking the form

$$H = \frac{1}{2} E_J \int d^2 r \, |\nabla \phi(\mathbf{r})|^2 \, . \tag{4}$$

Although the Gaussian model does not have long-range order because of the ubiquitous spin-wave excitations, which is the Goldstone mode, it indeed possesses quasi-long-range order at any temperature. In contrast, the XY model described by Eq. (3) also allows vortex excitations, destroying quasi-long-range order at $T > T_c$. The vortex charge, or the vorticity, n is defined from the line integral of the phase difference according to

$$\oint \nabla \phi \cdot d\mathbf{l} = 2\pi n, \tag{5}$$

and has the value $n = \pm 1$ for a single vortex/antivortex of unit charge. If a vortex with the vorticity n is located at the origin ($\mathbf{r} = 0$), the phase $\phi(\mathbf{r})$ at position $\mathbf{r}$ is simply given by $\phi(\mathbf{r}) = n\theta(\mathbf{r})$, where $\theta(\mathbf{r}) \equiv \tan^{-1}(y/x)$ with $\mathbf{r} = (x, y)$. At the vortex position ($\mathbf{r} = 0$), the azimuthal angle θ is undefined and thus the phase ϕ is also undetermined. This implies that $|\Psi(\mathbf{r}{=}0)| = 0$ and that the vortex excitation is a non-perturbative manifestation of the amplitude fluctuation.

The creation of a single vortex in the system with the linear size R costs the energy

$$E_v = \frac{1}{2} E_J \int d^2 r |\nabla \phi|^2 = \frac{E_J}{2} \int d^2 r \frac{1}{r^2} = \pi E_J \ln \left(\frac{R}{\xi_0} \right) + E_{\rm core}, \tag{6}$$

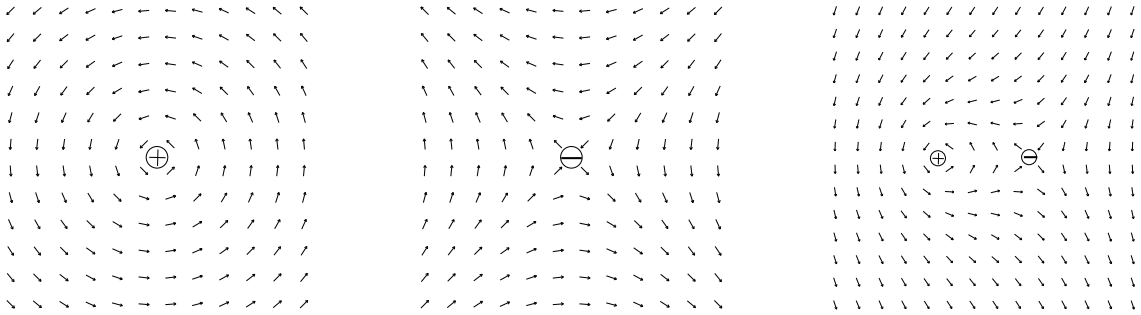

Figure 2: Topological excitations in the 2D XY model: (a) a single vortex, (b) an antivortex, and (c) a vortex-antivortex pair. The line integral of the phase difference around a single vortex/antivortex results in $\oint \nabla\phi \cdot d\mathbf{l} = 2\pi n$ with $n = \pm 1$. Directions of the arrows represent the phase values, e.g., the arrow in the positive x direction corresponds to $\phi = 0$.

where ξ_0 is the size of the vortex core (i.e., $|\Psi| \approx 0$ for $r \lesssim \xi_0$) and $E_{\rm core}$ is the vortex core energy. As the system size R becomes larger, Eq. (6) shows that the creation of a single isolated vortex costs a huge amount of energy and becomes energetically impossible. However, a vortex-antivortex pair separated by distance r can be created spontaneously by thermal fluctuations since it only costs the finite energy

$$E_p = 2\pi E_J \ln\left(\frac{r}{\xi_0}\right) + 2E_{\rm core}. \tag{7}$$

It should be noted that the logarithmic potential in Eq. (7) has the same form as the electrostatic Coulomb potential in two dimensions, which suggests that vortices can be treated as Coulomb charges [7]. At low temperatures, vortices energetically favor the formation of vortex-antivortex bound pairs instead of being free vortices. As the temperature is raised, the entropy contribution to the free energy becomes dominant, inducing dissociation of vortex pairs to free vortices. This can easily be seen from the consideration of the free energy cost to create a single free vortex. The energy contribution ΔE is simply the energy cost in Eq. (6). Taking into account the entropy contribution ΔS given by the logarithm of the number of accessible states to put a single vortex in the system, $\Omega \approx R^2/\xi_0^2$, we obtain the Free energy cost ΔF

$$\Delta F = \Delta E - T\Delta S = (\pi E_J - 2k_B T)\ln\left(\frac{R}{\xi_0}\right). \tag{8}$$

Consequently, we have $\Delta F > 0$ for $T < T_c \equiv (\pi/2)E_J/k_B$ and $\Delta F < 0$ otherwise. This indicates that free vortices cannot be created spontaneously at low temperatures while in the high-temperature phase vortex pairs dissociate to become free vortices.

To be more systematic, one may apply the dual transformation to the 2D XY

model [9], and obtain the vortex Hamiltonian:

$$H = 2\pi^2 E_J \sum_{\mathbf{R},\mathbf{R}'} n(\mathbf{R}) G(\mathbf{R},\mathbf{R}') n(\mathbf{R}'), \tag{9}$$

apart from the spin-wave contribution. Here $n(\mathbf{R})$ is the vortex charge defined on the dual lattice site $\mathbf{R}$, and $G(\mathbf{R},\mathbf{R}')$ is the lattice Coulomb Green's function. The diverging diagonal components, $G(\mathbf{R},\mathbf{R}) = \infty$, imposes the neutrality condition $\sum_{\mathbf{R}} n(\mathbf{R}) = 0$. Monte-Carlo simulations aided by the finite-size scaling analysis from the Kosterlitz-Thouless renormalization-group equation has yielded $k_B T_c/E_J \approx 0.89$ [10].

In the presence of an external magnetic field, one can adopt the minimal coupling scheme and simply replace ∇ in the GL free energy by $\nabla + i(e/c)\mathbf{A}$ with the corresponding vector potential $\mathbf{A}$, which restores gauge invariance. This leads to the Hamiltonian for the frustrated XY model:

$$H = -E_J \sum_{\langle i,j \rangle} \cos(\phi_i - \phi_j - A_{ij}), \tag{10}$$

where the magnetic bond angle is given by the line integral $A_{ij} \equiv (2\pi/\Phi_0) \int_i^j \mathbf{A} \cdot d\mathbf{l}$ with the flux quantum $\Phi_0 \equiv hc/2e$. The summation of A_{ij} around a plaquette yields

$$\sum_p A_{ij} = 2\pi(\Phi/\Phi_0) \equiv 2\pi f, \tag{11}$$

where Φ is the magnetic flux through the plaquette and accordingly, the *frustration* parameter f corresponds to the number of flux quanta per plaquette. When a uniform external magnetic field is applied, f is constant and we obtain the uniformly frustrated XY model. In this case it is sufficient to consider f in the interval $0 \le f \le 1/2$, owing to the invariance of the Hamiltonian under the transformations $f \to -f$ and $f \to f + 1$. When f is a rational number, i.e., $f = p/s$ with p and s being relative primes, the system possesses not only the U(1) symmetry but also the discrete $\mathrm{Z_s}$ symmetry, and can exhibit long-range order at finite temperatures even in two dimensions. The chirality $C(\mathbf{R})$, which is a useful variable for the description of the possible long-range order in the uniformly frustrated XY model, is given by the plaquette sum of the gauge-invariant phase difference:

$$C(\mathbf{R}) \equiv \frac{1}{2\pi} \sum_p (\phi_i - \phi_j - A_{ij}), \tag{12}$$

where the phase difference $(\phi_i - \phi_j - A_{ij})$ is defined modulo 2π in the range $(-\pi, \pi]$. The chirality $C(\mathbf{R})$ is related to the vorticity or the vortex charge $n(\mathbf{R})$ via the relation

$$C(\mathbf{R}) = n(\mathbf{R}) - f. \tag{13}$$

In the uniformly frustrated XY model with rational f, it is generally believed that there emerges long-range order in the chirality, associated with the discrete symmetry, at sufficiently low temperatures. The dual transformation to the partition

function for the uniformly frustrated XY model results in the Coulomb gas Hamiltonian for fractional charges:

$$H = 2\pi^2 E_J \sum_{\mathbf{R},\mathbf{R}'} [n(\mathbf{R}) - f] G(\mathbf{R}, \mathbf{R}') [n(\mathbf{R}') - f]. \tag{14}$$

Although the above Hamiltonian (14) appears similar to that for the unfrustrated XY model, given by Eq. (9), direct application of the renormalization-group formalism is not possible since the ground state consists of the $s \times s$ superlattice formed by vortices.

It has been shown that the GL type free-energy functional approach is very useful, with the help of the Hubbard-Stratonovich transformation applied to the Hamiltonian (10) [11]. With the definition

$$J_{ij} \equiv \begin{cases} E_J, & \text{if } i \text{ and } j \text{ are neighboring sites,} \\ 0, & \text{otherwise,} \end{cases} \tag{15}$$

the free energy functional reads

$$F[\Psi] = \frac{1}{2} \sum_{i,j} \Psi_i^* P_{ij}^{-1} \Psi_j - \frac{1}{4} \sum_i |\Psi_i|^2 + \frac{1}{64} \sum_i |\Psi_i|^4, \tag{16}$$

where the interaction matrix is given by $k_B T P_{ij} \equiv J_{ij} e^{-iA_{ij}}$. If we neglect fluctuations, the order parameter Ψ_i which minimizes the free energy functional F determines the critical behavior. Near the transition temperature, where $|\Psi_i| \approx 0$, we can further simplify the expression of the free energy minimum to obtain the following equation:

$$\sum_j J_{ij} e^{-iA_{ij}} \Psi_j = 2 k_B T \Psi_i. \tag{17}$$

Interestingly, with the identification of Ψ_i with the wave function at position i, Eq. (17) may be regarded as the quantum mechanical Schrödinger equation describing a tight-binding particle of charge $2e$ in the external magnetic field corresponding to the vector potential $\mathbf{A}$ [12]. It is also to be noted that the same equation describes the charge-density wave with the filling factor f.

In the case of a 2D square array, the position i of the superconducting grain is labelled by the x and y coordinates: $i = (m, l)$, where we have set the lattice constant $a \equiv 1$ to make m and l be integers. Employing the Landau gauge $\mathbf{A} = Bx\hat{\mathbf{y}}$, we reduce Eq. (17) to Harper's equation [12]:

$$\psi_{m+1} + \psi_{m-1} + V \cos(2\pi f m + \theta) \psi_m = \epsilon \psi_m, \tag{18}$$

where new variables $\psi_m \equiv e^{il\theta} \Psi_{m,l}$ have been introduced. Since J_{ij} in Eq. (15) is isotropic, we have the isotropic coupling $V = 2$, and the energy eigenvalue ϵ corresponds to $2k_B T/E_J$. The energy spectrum of Harper's equation has been intensively studied: When f is a rational, written as $f = p/s$, the Bloch theorem is applicable and gives the extended wave function ψ_m, with s energy bands. In the superconducting array, this corresponds to the superconducting state, where global phase

coherence is present. On the other hand, for an irrational f, all eigenstates are extended and localized for $V < 2$ and for $V > 2$, respectively; in between ($V = 2$) eigenstates are known to be critical.

We now consider the fully frustrated system ($f = 1/2$), which is the simplest among the uniformly frustrated XY models. In this case there exists two-fold degeneracy, which cannot be connected to each other via global rotation of spins, as illustrated in Fig. 3(a). It corresponds to the Z_2 symmetry, present in addition to the continuous degeneracy described by the U(1) symmetry. The Z_2 symmetry in the fully frustrated XY (FFXY) model is more clearly manifested by the two kinds of antiferromagnetic chirality ordering shown in Fig 3(b). The coexistence of the two kinds of symmetry naturally leads to the possibility of two types of phase transitions, a BKT type one corresponding to the U(1) symmetry and an Ising-like one associated with the Z_2 symmetry. In this system there exist two types of excitations shown in Fig. 4. The ($+1/2$, $-1/2$) chirality pair excitation, illustrated in Fig. 4(a), arises form the interchange of ($+1/2$) and ($-1/2$) chiralities and is expected to play the role similar to that of the vortex-antivortex pair in the pure XY model, breaking the quasi-long-range order for phases. On the other hand, the domain wall excitation, which is generated by the inversion of chirality in a finite domain as shown in Fig. 4(b), is believed to destroy the antiferromagnetic chirality order. The two transitions, however, are likely to take place at very close temperatures or even simultaneously, since the spin and the chirality degrees of freedom are not independent of each other. The phase transitions in the FFXY model have been studied by numerical simulations [13] and also by the renormalization-group analysis [14]. Although there is now growing consensus that the system has two transitions at distinct temperatures, nature of the transition is still in controversy.

As the frustration parameter f is varied, the symmetry of the frustrated XY model changes discontinuously. For example, an infinitesimal change of f from $f = 1/2$ leads to $f = p/s$ with the denominator s drastically different from 2. This in turn changes the symmetry of the system, resulting in a transition of very different nature. Particularly, in the case of irrational frustration, the possibility of a structural glass phase without intrinsic random disorder has been a long standing problem. It is still controversial whether there exists a finite-temperature transition in the system [15, 16]. The recent study, which has demonstrated the presence of novel finite-size effects and a glass transition at zero temperature, may be a resolution to the problem [17]. Another interesting model, the XY gauge glass model, where the magnetic bond angle A_{ij} are quenched random variables, has also drawn much attention since it may be related with the vortex glass phase in high-T_c superconductors [18]. It is generally accepted that in three dimensions the glass transition occurs at a finite temperature [19]. In two dimensions, on the other hand, it has been shown via two-replica representation that there is no long-range glass ordering [20]. Nevertheless the interesting possibility of quasi-long-range glass order at finite temperatures has been suggested recently [21].

Similarly to the persistent current due to the Aharonov-Bohm effect in electron systems, superconducting arrays with non-simply connected geometry such as the Josephson-junction necklace in one dimension [22] and the 2D array on the surface

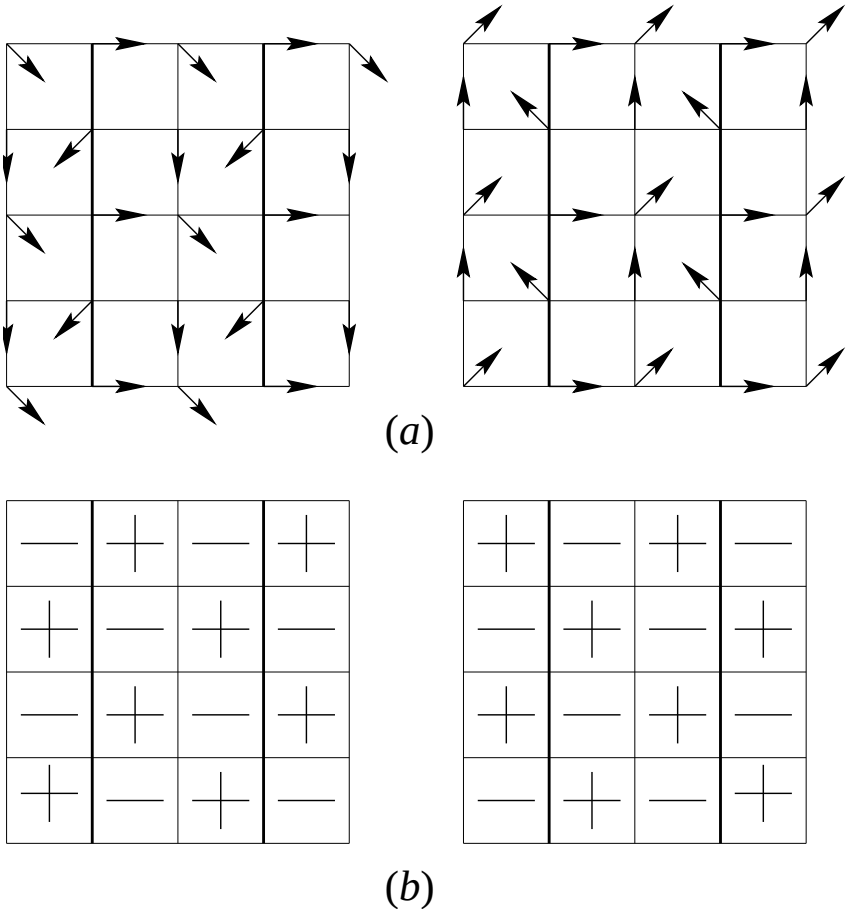

Figure 3: (a) Spin configurations in the two ground states of the fully frustrated XY model on a square lattice. All other ground states can be obtained from either of them via appropriate (global) spin rotations, but the two ground states cannot be transformed to each other by any global rotation. Here we have used the Landau gauge. The thick lines represent antiferromagnetic bonds while thin lines denote ferromagnetic bonds. (b) Chirality configurations in the two ground states. (+) and (−) in each plaquette represent the positive (+1/2) and negative (−1/2) chirality, respectively. The vortex charge is +1 at (+) plaquettes and 0 at (−) plaquettes.

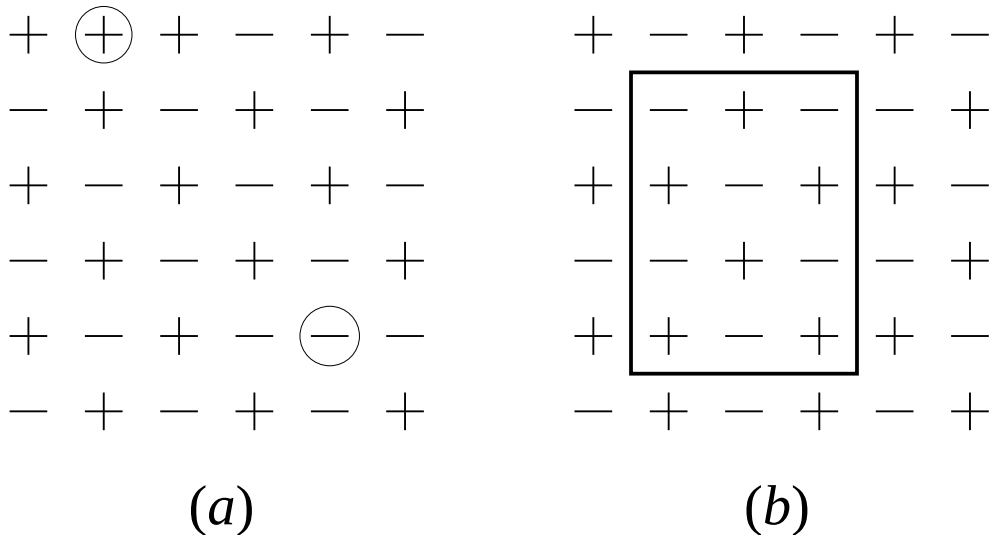

Figure 4: Two types of excitations in the fully frustrated XY model: (a) $(+1/2, -1/2)$ chirality pair excitation and (b) domain-wall excitation.

of a cylinder or a torus [23] has been shown to carry persistent currents. In the presence of the external magnetic flux Φ penetrating the center of the non-simply connected geometry, the persistent current circulating the system at $T = 0$ is given by

$$I = \frac{2e}{h} \frac{\partial E}{\partial(\Phi/\Phi_0)}, \tag{19}$$

where the ground state energy E can be obtained from Eq. (10) or Eq. (18). In general, like other physical quantities, the persistent current shows periodicity in the flux Φ with the period Φ_0. It has also been pointed out that a 2D system can display other fractional periodicity [23].

Theoretical study of dynamic properties of superconducting arrays, for example, current-voltage (I-V) characteristics, resistance, complex conductivity, and noise spectra, is particularly important in relation with experiments. For the investigation of these dynamic properties, the resistively-shunted junction (RSJ) dynamic model as well as the time-dependent Ginzburg-Landau (TDGL) model is frequently used [24]. In the RSJ model, the equations of motion are obtained from the current conservation rule applied to each grain: The sum of the Josephson supercurrent (I_s), the resistive current through shunt resistance (R), and the thermal noise current (L) should be equal to the external current source (I_i) attached to grain i. Using the Josephson relations for the junction between the grains i and j, $I_s = I_c \sin(\phi_i - \phi_j)$ and $d(\phi_i - \phi_j)/dt = 2eV_{ij}/\hbar$ with the voltage drop V_{ij} across the junction, one obtains the basic equation for the RSJ model:

$$\frac{\hbar}{2eR} \frac{d\phi_i}{dt} = \sum_j G_{ij} \left[I_j - I_c {\sum_k}' \sin(\phi_j - \phi_k) - L_{ij} \right], \tag{20}$$

where G_{ij} is the lattice Coulomb Green's function. It is defined by ${\sum_j}'(\phi_i - \phi_j) = \sum_j G_{ij}^{-1} \phi_j$ with the primed summation performed over nearest neighboring sites,

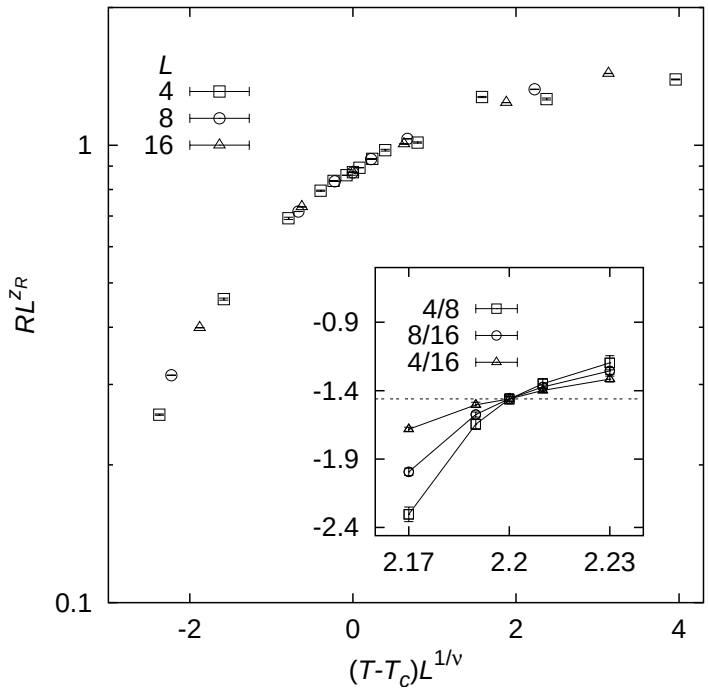

Figure 5: The scaling curve for resistance R for the 3D XY model with the RSJ dynamics. The parameters used are $z = 1.46$ and $T_c = 2.20$, determined by the intersection point shown in the inset, together with the critical exponent $\nu = 0.67$ expected for the 3D XY model (adopted from Ref. [27]).

which gives the same form as that in Eq. (9). The thermal noise current L_{ij} from i to j satisfies

$$\langle L_{ij}(t+\tau)L_{ij}(t)\rangle = \frac{2k_BT}{R}\delta(\tau)\left(\delta_{ik}\delta_{jl} - \delta_{il}\delta_{jk}\right) \tag{21}$$

with the Dirac delta function $\delta(\tau)$ and the Kronecker delta δ_{ik}. A practically useful boundary condition, termed the fluctuating twist boundary conditions (FTBC) [25], has been generalized to dynamic equations of motion [24]. In FTBC, an additional variable, called the twist variable, $\mathbf{\Delta} = (\Delta_x, \Delta_y)$ is introduced through the change of variables: $\phi_i \rightarrow \phi_i + \mathbf{r}_i \cdot \mathbf{\Delta}$ for the ith site at the position $\mathbf{r}_i$. The equation of motion for $\mathbf{\Delta}$ is then obtained from the condition of the global current conservation, i.e., the summation of all currents in each direction should be identically zero at any time t. The FTBC have been widely used to study various dynamic behaviors such as I-V characteristics, Shapiro steps, critical currents, and so on. The conventional boundary conditions in the presence of external currents, consisting of the free boundary condition along the current direction and the periodic boundary condition in the perpendicular direction, have been shown to cause much larger boundary effects than the FTBC [26].

The dynamic critical behaviors have been studied numerically via various dynamic simulations and analytically by investigating the stationary solution of the Fokker-Planck equation, obtained from the above set of Langevin-type dynamic equations [29]. The dynamic scaling hypothesis relates the I-V exponent a to the

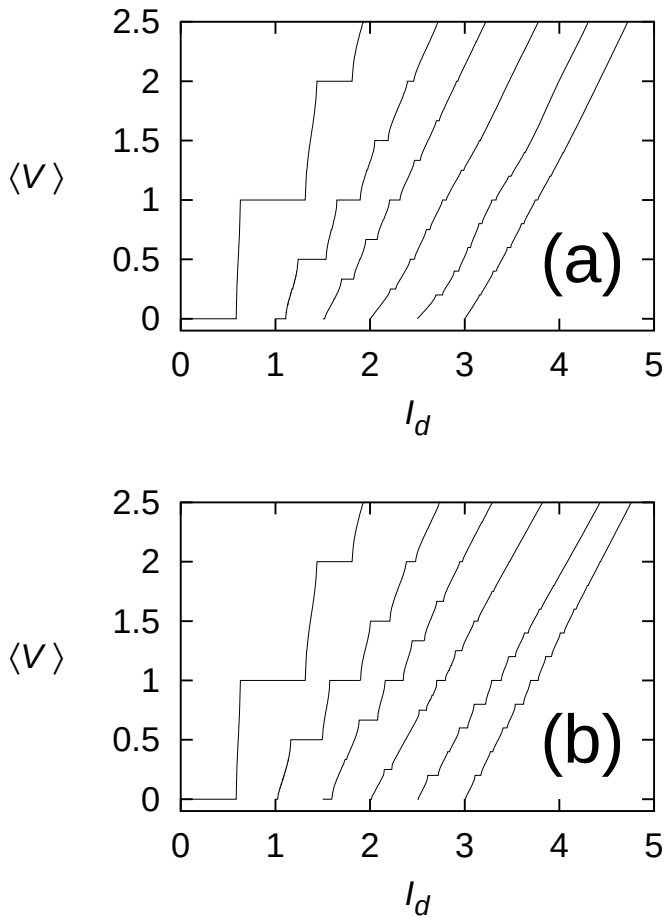

Figure 6: Fractional giant Shapiro steps observed for (a) RSJ and (b) TDGL dynamics. (The figure is from Ref.[28].)

dynamic critical exponent z via $a = z + 1$ in the limit of small currents [30]. There have been two different proposals on the temperature dependence of z, one by Ambegaokar *et al.* [31] and the other by Minnhagen *et al.* [32]. Although both give the same prediction at T_c, i.e., $z = 2$ and $a = 3$ as $T \to T_c$ from below, the value of z increases faster in the latter, as T is lowered. Many existing numerical simulations are in favor of the latter prediction [24, 33] although there are some exceptions [34]. Underlying discrete lattice structure of the array introduces effective pinning of vortices. It has been shown that the lattice effects become insignificant at small currents, suggesting that the dynamic critical behavior obtained from simulations on discrete lattices is universal, not depending on the details of the discretization [35]. This suggests that even the continuum 2D superconducting films should have the same exponent [36]. The dynamic critical behavior of the three-dimensional (3D) XY model have also been studied and the finite-size scaling of the resistance has yielded $z \approx 1.5$ and $k_B T_c/E_J \approx 2.20$ (see Fig. 5).

At zero temperature, an $L \times L$ square array with $f = p/s$, driven externally by the combined direct and alternating currents (with frequency ω), exhibits giant

Shapiro steps at time-averaged voltages

$$\langle V \rangle = \left(\frac{n}{s}\right) \frac{\hbar \omega L}{2e} \tag{22}$$

with n being positive integers. Topological invariance of such Shapiro steps has been suggested [38]; topological quantization is also important in other physical phenomena, e.g., vorticity quantization in superfluids and the quantum Hall effect. The Shapiro steps have also been found with the TDGL dynamics (see Fig. 6), which apparently implies that existence of steps does not depend on details of dynamics. This reflects their topological origin [28]. Particularly, it has been reported that the I-V characteristics of the frustrated XY model possesses the devil's staircase structure, i.e., there exist voltage steps at every fractional number [39]. When the array with non-simply connected geometry is driven by external time-oscillating magnetic flux, the Shapiro resonance, which is topological quantization of the magnetic flux, has also been suggested [40].

As the temperature is raised, thermal fluctuations have been shown to lead to other interesting phenomena such as the stochastic resonance [37] (see Fig. 7) and dynamic phase transitions, if the system is driven in an appropriate way. The relation between the flux-noise spectrum and the complex impedance has also been studied and the experimental results on high-T_c materials have been successfully explained by numerical dynamic simulations of superconducting arrays at finite temperatures [41].

3 QUANTUM ARRAYS

In superconducting arrays, there are three competing energy scales: the charging energy E_C, the Josephson energy E_J, and the thermal energy $k_B T$. When E_C is sufficiently small compared with E_J, one can describe the system by means of classical statistical physics (see Sec. 2). On the other hand, arrays of ultra-small grains with the capacitance $C \approx 10^{-15}$F have become available via current fabrication techniques; in such a system E_C, inversely proportional to C, may not be neglected compared with E_J, and the quantum description with full consideration of the commutation relation between the charge and the phase variables is required. The Hamiltonian for this quantum array is given by [4]

$$\begin{aligned} H &= 2e^2 \sum_{i,j} (n_i - q_i) C_{ij}^{-1} (n_j - q_j) - E_J \sum_{\langle i,j \rangle} \cos(\phi_i - \phi_j - A_{ij}) \\ &\equiv H_c - E_J \sum_{\langle i,j \rangle} \cos(\phi_i - \phi_j - A_{ij}), \end{aligned} \tag{23}$$

where n_i in the charging energy term H_c represents the quantum mechanical number operator measuring the excessive charge on the ith grain in units of the Cooper pair charge $2e$. It satisfies the commutation relation

$$[n_i, \phi_j] = -i\delta_{ij}. \tag{24}$$

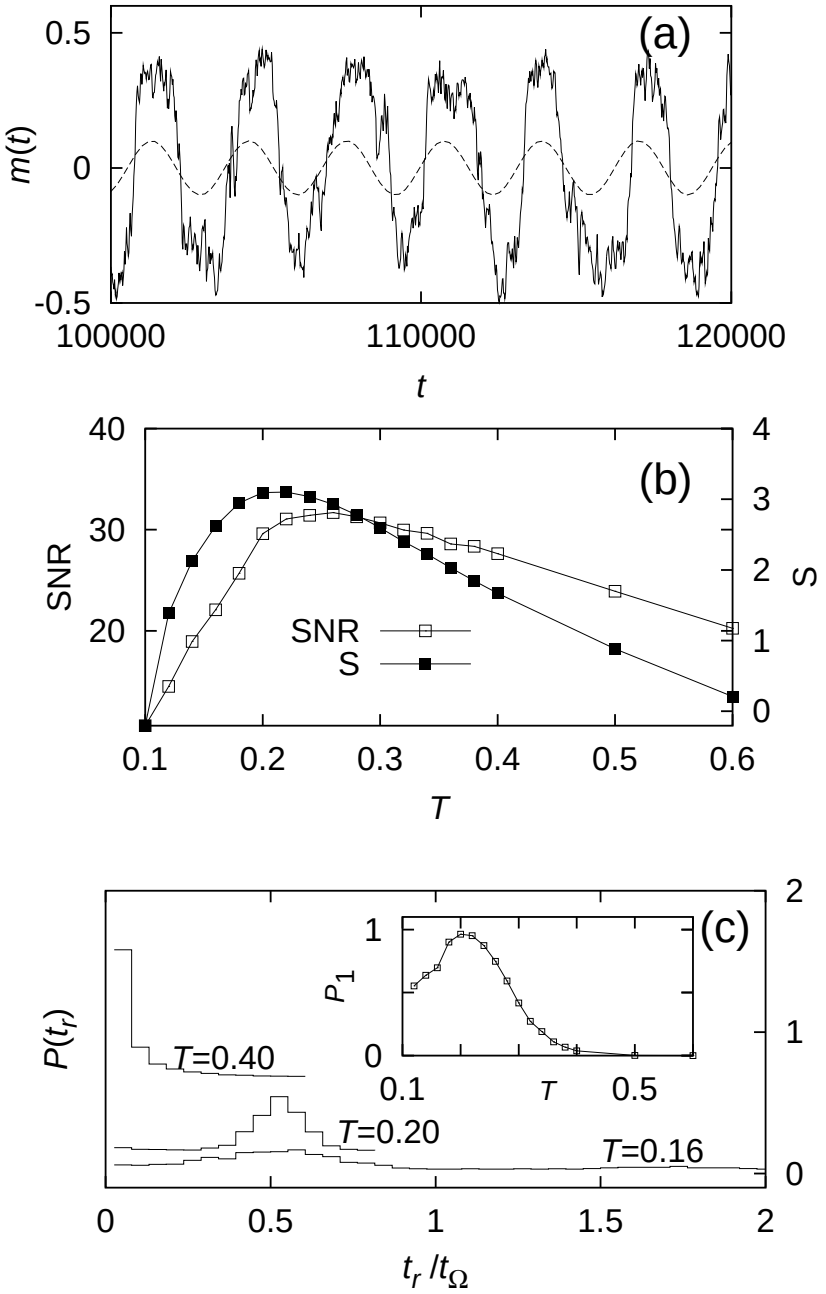

Figure 7: Stochastic resonance in the fully-frustrated Josephson-junction ladder array. (a) Time-series of the staggered magnetization $m(t)$; (b) signal-to-noise ratio SNR (left vertical scale); (c) residence-time distribution at several temperatures [inset: primary peak height] (adopted from Ref.[37].)

The gauge charge $Q_i \equiv -2eq_i$ can be induced by applying the gate voltage, and the capacitance matrix C_{ij} in general contains both the self-capacitance C_0 and the junction capacitance C_1:

$$C_{ij} = (C_0 + \gamma C_1)\delta_{ij} - C_1\delta_{ij'}, \tag{25}$$

where j' denotes the nearest neighbors of j and γ is the number of such neighbors or the coordination number. When $C_1 = 0$, the capacitance matrix has only diagonal components and the charging energy term corresponds to the standard kinetic energy term in a particle system. The Coulomb blockade effect due to the Cooper pair tunneling [4] can arise since the number operator can have only discrete integer eigenvalues and in this case the Josephson coupling term [the second term in Eq. (23)] acts as a tunneling Hamiltonian (see discussion below for the Bose-Hubbard model). The quantum superconducting array fabricated with only weak dissipation effects provides a typical example of macroscopic quantum systems, a testing ground of observing Schrödinger's cat.

The quantum Hamiltonian in Eq. (23) for superconducting arrays also draws much interest from the theoretical point of view, since it is related with other models such as the Bose-Hubbard model and the quantum spin model [42]. The former is obtained in the limit of very large $\langle n_i \rangle$:

$$H = -\sum_{i,j} t_{ij} e^{iA_{ij}} b_i^\dagger b_j + \sum_{i,j} n_i U_{ij} n_j - \sum_i (\mu + \nu_i) n_i, \tag{26}$$

where $b_i^\dagger / b_i$ is the boson creation/annihilation operator in the second quantization notation, t_{ij} and U_{ij} correspond to J_{ij} [see Eq. (15)] and C_{ij}^{-1}, respectively, and the chemical potential μ and the on-site potential ν_i are related to the gauge charge q_i. The first term, which corresponds to the Josephson coupling term in Eq. (23), annihilates a boson at site i and creates one at j, describing tunneling of bosons (Cooper pairs). In a similar way, one can also transform the Hamiltonian (23) to the quantum spin model:

$$H = -\sum_{i,j} t_{ij}(S_i^x S_j^x + S_i^y S_j^y) + \sum_{i,j} U_{ij} S_i^z S_j^z - h \sum_i S_i^z, \tag{27}$$

where $\mathbf{S}_i = (S_i^x, S_i^y, S_i^z)$ is the spin operator and the external field h is related to the gauge charge in Eq. (23). In an appropriate limit, the quantum spin model can also be related to the charge-density wave system with the kinetic energy term and the coupling between chains included.

In the above quantum systems, not only thermal fluctuations but also quantum fluctuations play important roles. Furthermore, the frustration effects due to both the external magnetic flux and the external gauge charge can result in many interesting behaviors such as thermodynamic and quantum phase transitions separating the superconducting (S), the normal (N), and the insulating (I) phases. When the charging energy is sufficiently small, the Josephson energy ensures that the system at zero temperature establishes global phase coherence to become a superconductor. In the opposite case of small Josephson coupling energy, the ground state exhibits

charge ordering, which corresponds to the Mott insulating phase. Accordingly, as the ratio of the charging energy to the Josephson energy is varied, a superconductor-insulator (S-I) transition of purely quantum mechanical nature takes place. As the temperature is raised, thermal fluctuations intervene and a variety of interesting critical behaviors are observed as the dimensionality of the system is changed, as the capacitance matrix is varied, and as the dissipation effects due to the shunt resistance and quasi-particle tunneling are considered.

It is often convenient to employ the path integral formalism in the study of a quantum phase transition. In the self-charging limit ($C_1 = 0$) and in the absence of the gauge charge ($q_i = 0$), one can express the charging energy term in the Euclidean action as the form of the Josephson coupling energy, with the phase difference taken along the imaginary time axis. At zero temperature, the Euclidean action contains the integration over the imaginary time τ from zero to $\beta \equiv 1/k_B T\,(\rightarrow \infty)$ and one can interpret the Euclidean action in d dimensions as the effective classical Hamiltonian for the (classical) system in d+1 dimensions:

$$\beta H_{\rm eff} = -K \sum_{\langle \mathbf{r},\mathbf{r}' \rangle} \cos(\phi_{\mathbf{r}} - \phi_{\mathbf{r}'} - A_{\mathbf{r}\mathbf{r}'}), \tag{28}$$

where the lattice site $\mathbf{r} \equiv (i, \tau)$ has been defined in d+1 dimensions and the effective coupling strength is given by $K \equiv \sqrt{E_J/E_C}$ with the charging energy $E_C \equiv 4e^2/C_0$. Consequently, the 1D quantum superconducting array at zero temperature can be considered as the 2D classical array represented by the 2D classical XY model. In the former the parameter $1/K = \sqrt{E_C/E_J}$ controls the strength of quantum fluctuations and takes the role of the temperature T controlling the strength of thermal fluctuations in the latter. From the known result $k_B T_c/E_J \approx 0.89$ for the 2D classical XY model, one concludes that the 1D quantum array should have a quantum transition of the BKT nature at $E_C/E_J \approx 0.8$ between the superconducting and the insulating phases. Similarly, the 2D array without frustrations ($f = q = 0$) at zero temperature is mapped to the 3D classical XY model and thus the superconductor-insulator transition in the former has the same nature as the bulk superfluids like Helium. At finite temperatures, thermal fluctuations give rise to a superconducting-normal (S-N) transition in place of the S-I transition due to quantum fluctuations. The quantum fluctuations in this case renormalize effectively the Josephson coupling and lower the transition temperature. The appearance of a reentrant transition (from the normal to the superconducting and then to the normal phase again as T is lowered) in the presence of intermediate quantum fluctuations has been suggested but still remains as a source of controversy [43]. In addition, dissipation, which has been shown to suppress the effects of quantum fluctuations [44], requires more detailed study with the allowed charge states taken into account. The gauge charge q also affects the phase transition in the system and has been studied by using the mean-field approximation [42] and recently by the renormalization-group method [45].

When the capacitance matrix in Eq. (25) has only the off-diagonal elements, i.e., $C_0 = 0$ (the nearest-neighbor charging limit), C_{ij}^{-1} can be written in the form G_{ij}/C_1 with the lattice Coulomb Green's function G_{ij}, and the charging energy term

H_c in Eq. (23) has exactly the same form as the classical Hamiltonian in Eq. (14). Consequently, the charging energy term and the Josephson energy term takes the same form, which reflects the duality in the system [46]. For a 2D array in the presence of uniform gauge charges, we define the charging energy $E_C \equiv 4e^2/C_1$, and obtain

$$H = \frac{1}{2} E_C \sum_{i,j} (n_i - q) G_{ij} (n_j - q) - E_J \sum_{\langle i,j \rangle} \cos(\phi_i - \phi_j - A_{ij}), \tag{29}$$

which, apart from spin-wave fluctuations, can be transformed into the following vortex representation

$$H = 2\pi^2 E_J \sum_{i,j} (n_i - f) G_{ij} (n_j - f) - \frac{E_C}{4\pi^2} \sum_{\langle i,j \rangle} \cos(\phi_i - \phi_j - A_{ij}). \tag{30}$$

Here the number operator n_i, measuring the vortex charge at dual lattice site i, and the phase ϕ_i of the vortex again constitute quantum mechanical conjugate variables, whereas the bond angle A_{ij} satisfies $\sum_p A_{ij} = 2\pi q$ [note the similarity to Eq. (11)]. Equations (29) and (30) are related via $E_C \Leftrightarrow 4\pi^2 E_J$ and manifest clearly the duality between Cooper pairs and vortices. At zero temperature, for $E_C \ll E_J$, vortices behave as well-defined particles and according to Eq. (30) form a superlattice structure in the ground state; the system is superconducting with vortices frozen on the dual lattice. In the opposite limit of $E_C \gg E_J$, Cooper pairs are well-defined particles and form charge lattice structure, which is the Wigner crystal. The system behaves as an insulator with charges pinned at lattice sites. Therefore, one can expect the S-I transition when E_C and E_J are comparable with each other. For $f = q$, in particular, the duality in the system predicts that the S-I transition takes place at the self-dual point $E_C = 4\pi^2 E_J$. Near the S-I transition, Cooper pairs or vortices have sufficiently large kinetic energies and the charge lattice or the vortex lattice tends to melt, forming strongly-correlated quantum fluids. Berry's phase acquired by a vortex in motion indicates that the vortex as well as a Cooper pair behaves as a boson [47]. However, the hard-core nature of a vortex makes it possible to apply the Jordan-Wigner transformation, which transforms vortices into fermions in appropriate gauge fields. The resulting possibility of the quantum Hall effect has thus been suggested as f and q are varied [47, 48].

At finite temperatures, as thermal fluctuations grow stronger, charges (Cooper pairs) or vortices become free and the system enters into the normal state with finite resistance. Accordingly, as E_C/E_J is varied at finite temperatures, expected is either the superconducting-normal transition, where vortex dipole pairs unbind to become free vortices, or the insulating-normal transition associated with charge dipole unbinding. For the relatively simple case of $f = q = 0$, quantum Monte Carlo simulations [49], perturbation expansion [50], and renormalization-group analysis combined with the variational method [51], have shown the existence of transitions, which was confirmed by experiments [2]. In the more general case with finite values of f and q, various forms of C_{ij}, and dissipation effects included, it has been partially found that there exist very complex phase boundaries. Of particular interest is the possibility of the supersolid phase, where both diagonal and off-diagonal long range order coexist [52].

The duality between charges and vortices suggests many interesting possibilities. Similarly to localization of charges, localization of quantum vortices may be expected in the presence of random disorder. When the superconducting array with a non-simply connected geometry is penetrated by an external magnetic flux, the Aharonov-Bohm effect has been shown to induce persistent currents (see Sec. 2). In parallel with this, one can also expect the quantum interference of vortices (via the Aharonov-Casher effect) in the presence of external gauge charge, which plays the role of the magnetic flux in the above-mentioned Aharonov-Bohm effect [22, 53]. Such interference of quantum vortices then gives rise to the persistent voltage:

$$V = \frac{1}{2e}\frac{\partial E}{\partial q}. \tag{31}$$

The resulting Bloch oscillation of the persistent voltage has the periodicity $q = 1$; however, it can also display other fractional periodicity [53], similarly to the fractional quantum Hall effect. Furthermore, in the presence of alternating currents, the gauge charge oscillates in time and another topological quantization, the inverse giant Shapiro step, which constitutes a counterpart of the giant Shapiro step for Cooper pairs, has been predicted [54].

4 Conclusions

Superconducting arrays possess rich physics, exhibiting very diverse phenomena including diagonal and off-diagonal long range order, quasi-long-range order, Berry's phase, the quantum Hall effect, quantum fluctuations and dissipation effects, quantum phase transitions, mode locking, and stochastic resonances. Also suggested recently is the possibility of observing excitons and cotunneling phenomena in coupled arrays [55] and the Bose-Einstein condensation. These various phenomena are usually studied through the use of path integral, dual transformation, renormalization-group analysis, replica trick, stochastic equations, bosonization, perturbative expansion, variational approach, projection techniques, and the Bethe ansatz. In addition to these analytic approaches, it has become essential to use various simulational techniques like classical and quantum Monte Carlo simulations and numerical integration techniques of stochastic equations. Consequently, superconducting arrays are one of the most convenient systems for the study of quantum coherence, from both theoretical and experimental points of view. In particular, it is manifested that such interesting phenomena as topological quantization, fractional charges, gauge interactions, and symmetry breaking emerge as a result of the cooperativity between the many degrees of freedom in the array system.

References

[1] H.A. Cerdeira, B. Kramer, and G. Schön, *Quantum Dynamics of Submicron Structures* (Kluwer, Dordrecht, 1995).

[2] See, e.g., C. Giovannela and M. Tinkham (eds.) *Macroscopic Quantum Phenomena and Coherence in Superconducting Networks* (World Scientific, Singapore, 1996); C. Giovannela and C.J. Lambert, (eds.) *Lectures on Superconductivity in Networks and Mesoscopic Systems* (American Institute of Physics, New York, 1998); Physica B, **222** (1996) 253.

[3] V.L. Berezinskii, Zh. Eksp. Teor. Fiz., **59** (1970) 907 [Sov. Phys. JETP, **32** (1971) 493]; J.M. Kosterlitz and D.J. Thouless, J. Phys. C, **6** (1973) 1181; J.M. Kosterlitz, *ibid.*, **7** (1974) 1046.

[4] G. Schön and A.D. Zaikin, Phys. Rep., **198** (1990) 237.

[5] M. Tinkham, *Introduction to Superconductivity*, 2nd edition (McGraw-Hill, New York, 1996).

[6] A.P. Gottlob and M. Hasenbusch, Physica A, **201** (1993) 593.

[7] P. Minnhagen, Rev. Mod. Phys., **59** (1987) 1001.

[8] N.D. Mermin and H. Wagner, Phys. Rev. Lett., **17** (1966) 1133.

[9] J.V. José, L.P. Kadanoff, S. Kirkpatrick, and D.R. Nelson, Phys. Rev. B, **16** (1977) 1217.

[10] H. Weber and P. Minnhagen, Phys. Rev. B, **37** (1988) 5986.

[11] M.Y. Choi and S. Doniach, Phys. Rev. B, **31** (1985) 4516.

[12] M.Y. Choi, in *Discrete Phenomena in Mathematics and Physics*, edited by D.P. Chi (Pure Math. Res. Asso., Seoul, 1991) pp 151-164; in *Progress in Statistical Mechanics*, edited by C.-K. Hu (World Scientific, Singapore, 1988), p. 385; W.Y. Shih and D. Stroud, Phys. Rev. B, **28** (1983) 6575.

[13] D.B. Nicolaides, J. Phys. A, **24** (1991) L231; G. Ramirez-Santiago and J.V. José, Phys. Rev. Lett., **68** (1992) 1224; J. Lee, J.M. Kosterlitz, and E. Granato, Phys. Rev. B, **43** (1991) 11531; J.-R. Lee, *ibid.*, **49** (1994) 3317; S. Lee and K.-C. Lee, *ibid.*, **49** (1994) 15184; P. Olsson, Phys. Rev. Lett., **75** (1995) 2758.

[14] M.Y. Choi and D. Stroud, Phys. Rev. B, **32** (1985) 5773; M. Yosefin and E. Domany, *ibid.*, **32** (1985) 1778; G.S. Jeon, S.Y. Park, and M.Y. Choi, *ibid.*, **55** (1997) 14088.

[15] M.Y. Choi, and D. Stroud, Phys. Rev. B, **32** (1985) 7532; E. Granato, *ibid.*, **54** (1996) R9655.

[16] T.C. Halsey, Phys. Rev. Lett., **55** (1985) 1018; R.W. Reid, S.K. Bose, and B. Mitrović, Phy. Rev. B, **54** (1996) R740; J. Phys. Condens. Matter, **9** (1997) 7141; B. Kim and S.J. Lee, Phys. Rev. Lett., **78** (1997) 3709; P. Gupta, S. Teitel, and M.J.P. Gingras, *ibid.*, **80** (1998) 105; C. Denniston and C. Tang, Phys. Rev. B, **60** (1999) 3163.

[17] S.Y. Park, M.Y. Choi, B.J. Kim, G.S. Jeon, and J.S. Chung, Phys. Rev. Lett., **85** (2000) 3484.

[18] D.S. Fisher, M.P.A. Fisher, and D.A. Huse, Phys. Rev. B, **43** (1991) 130.

[19] D.A. Huse and H.S. Seung, Phys. Rev. B, **42** (1990) 1059; M. Cieplak, J.R. Banavar, and A. Khurana, J. Phys. A, **24** (1991) L145; M. Cieplak, J.R. Banavar, M.S. Li, and A. Khurana, Phys. Rev. B, **45** (1992) 786.

[20] H. Nishimori, Physica A, **205** (1994) 1.

[21] M.Y. Choi and S.Y. Park, Phys. Rev. B, **60** (1999) 4070; B.J. Kim, *ibid.*, **62** (2000) 644.

[22] M.Y. Choi, Phys. Rev. B, **48** (1993) 15920.

[23] J. Yi and M.Y. Choi, Phys. Rev. B, **56** (1997) 2368. See also M.Y. Choi and J. Yi, Phys. Rev. B, **52** (1995) 13769

[24] B.J. Kim, P. Minnhagen, and P. Olsson, Phys. Rev. B, **59** (1999) 11506.

[25] P. Olsson, Phys. Rev. B, **46** (1992) 14598; **52** (1995) 4526.

[26] M.Y. Choi, G.S. Jeon, and M. Yoon, Phys. Rev. B, **62** (2000) 5357; B.J. Kim and P. Minnhagen, *ibid.*, **61** (2000) 7017.

[27] L.M. Jensen, B.J. Kim, and P. Minnhagen, Europhys. Lett., **49** (2000) 644.

[28] B.J. Kim and P. Minnhagen, Phys. Rev. B, **60** (1999) 588.

[29] S. Kim, M.Y. Choi, and J.S. Chung, J. Phys. A, **25** (1992) L1203.

[30] A.T. Dorsey, Phys. Rev. B **43** (1991) 7575.

[31] V. Ambegaokar, B.I. Halperin, D.R. Nelson, and E.D. Siggia, Phys. Rev. Lett., **40** (1978) 783; Phys. Rev. B, **21** (1980) 1806.

[32] P. Minnhagen, O. Westman, A. Jonsson, and P. Olsson, Phys. Rev. Lett., **74** (1995) 3672.

[33] H. Weber and H.J. Jensen, Phys. Rev. Lett., **78** (1997) 2620; H.-C. Chu and G.A. Williams, *ibid.*, **86** (2001) 2585; K. Holmlund and P. Minnhagen, Phys. Rev. B, **54** (1996) 523; B.J. Kim, *ibid.*, **63** (2001) 024503.

[34] M.V. Simkin and J.M. Kosterlitz, Phys. Rev. B, **55** (1997) 11646; Q.-H. Chen, L.-H. Tang, and P. Tong (unpublished).

[35] M. Yoon, M.Y. Choi, and B.J. Kim, Phys. Rev. B, **61** (2000) 3263.

[36] K. Medvedyeva, B.J. Kim, and P. Minnhagen, Phys. Rev. B, **62** (2000) 14531.

[37] B.J. Kim, M.-S. Choi, P. Minnhagen, G.S. Jeon, H.J. Kim, and M.Y. Choi, Phys. Rev. B, **63** (2001) 104506.

[38] M. Kvale and S.E. Hebboul, Phys. Rev. B, **43** (1991) 3720; M.Y. Choi, *ibid.*, **46** (1992) 564.

[39] S. Kim and M.Y. Choi, Europhys. Lett., **23** (1993) 217; S. Kim, B.J. Kim, and M.Y. Choi, Phys. Rev. B, **52** (1995) 13536.

[40] M.Y. Choi and J. Yi, Europhys. Lett., **35** (1996) 457.

[41] B.J. Kim and P. Minnhagen, Phys. Rev. B, **60** (1999) 6834; O. Festin, P. Svedlindh, B.J. Kim, P. Minnhagen, R. Chakalov, and Z. Ivanov, Phys. Rev. Lett., **83** (1999) 5567.

[42] A. van Otterlo, K.-H. Wagenblast, R. Baltin, C. Bruder, R. Fazio, and G. Schön, Phys. Rev. B, **52** (1995) 16176.

[43] E. Simánek, Phys. Rev. B, **23** (1981) 5762; **32** (1985) 500; K.B. Efetov, Zh. Eksp. Teor. Fiz., **78** (1980) 2017 [Sov. Phys. JETP, **51** (1980) 1015]; P. Fazekas, Z. Phys. B, **45** (1982) 215; J.V. José, Phys. Rev. B, **29** (1984) 2836; M.Y. Choi, and D. Stroud, *ibid.*, **32** (1985) 7173; S. Kim and M.Y. Choi, *ibid.*, **41** (1990) 111.

[44] S. Chakravarty, G.L. Ingold, S. Kivelson, and A. Luther, Phys. Rev. Lett., **56** (1986) 2303; E. Simánek and R. Brown, Phys. Rev. B, **34** (1986) 3495; S. Chakravarty, S. Kivelson, G.T. Zimanyi, and B.I. Halperin, *ibid.*, **35** (1987) 7256; A. Kampf and G. Schön, *ibid.*, **37** (1988) 5954; J. Choi and J.V. José, Phys. Rev. Lett. **62** (1989) 1904; S. Kim and M.Y. Choi, Phys. Rev. B, **42** (1990) 80.

[45] M.Y. Choi, S.W. Rhee, M. Lee, and J. Choi, Phys. Rev. B, **63** (2001) 094516.

[46] R. Fazio, A. van Otterlo, G. Schön, H.S.J. van der Zant, and J.E. Mooij, Helv. Phys. Acta, **65** (1992) 228.

[47] M.Y. Choi, Physica B, **222** (1996) 358.

[48] M.Y. Choi, Phys. Rev. B, **50** (1994) 10088; A. Stern, *ibid.*, **50** (1994) 10092; M.Y. Choi and J. Choi, *ibid.*, **63** (2001) 212503. See also A.A. Odintsov and Yu.V. Nazarov, Phys. Rev. B, **51** (1995) 1133.

[49] C. Rojas and J.V. José, Phys. Rev. B, **54** (1996) 12361.

[50] J.K. Freericks and H. Monien, Phys. Rev. B, **53** (1996) 2691; A.A. Odintsov, *ibid.*, **54** (1996) 1228.

[51] B.J. Kim and M.Y. Choi, Phys. Rev. B, **52** (1995) 3624.

[52] B.J. Kim, J. Kim, S.Y. Park, and M.Y. Choi, Phys. Rev. B, **56** (1997) 395.

[53] M.Y. Choi, Phys. Rev. Lett., **71** (1993) 2987; J. Yi, G.S. Jeon, and M.Y. Choi, Phys. Rev. B, **52** (1995) 7838.

[54] M.Y. Choi, Phys. Rev. B, **50** (1994) R13875.

[55] M.-S. Choi, M.Y. Choi, T.S. Choi, and S.-I. Lee, Phys. Rev. Lett., **81** (1998) 4240; M. Lee, M.-S. Choi, and M.Y. Choi, Phys. Rev. B, **60** (1999) 10455; M.-S. Choi, M.Y. Choi, and S.-I. Lee, J. Phys.: Condens. Matter, **12** (2000) 943.